2015

Energy absorption and impact response of GFRP reinforced concrete beams

M W. Goldston
University of Wollongong, mwg278@uowmail.edu.au

A M. Remennikov
University of Wollongong, alexrem@uow.edu.au

M N. Sheikh
University of Wollongong, msheikh@uow.edu.au

Publication Details

Goldston, M., Remennikov, A. M. & Sheikh, M. Neaz. (2015). Energy absorption and impact response of GFRP reinforced concrete beams. 3rd International Conference on Protective Structures (ICPS3) (pp. 168-176). Australia: University of Newcastle.

Energy absorption and impact response of GFRP reinforced concrete beams

Abstract

It has been demonstrated that glass fibre-reinforced polymer (GFRP) bars is a suitable alternative to traditional steel reinforcement in concrete structures. GFRP bars are a competitive reinforcing option in reinforced concrete members subjected to flexure and shear. GFRP has compelling physical and mechanical properties, corrosion resistance and electromagnetic transparency. The use of GFRP reinforcement is particularly attractive for structures that operate in aggressive environments, such as in coastal regions, or for buildings that host magnetic resonance imaging (MRT) units or other equipment sensitive to electromagnetic fields. However its behaviour under impact loading is not adequately known. This study involved testing a total of twelve GFRP Reinforced Concrete (RC) beams under static and impact loadings and analysing the effect of certain variables including longitudinal reinforcement ratio and concrete strength (normal and high strength). Experimental results confirm that beams with GFRP as internal reinforcement have extremely low post cracking bending stiffness. One noticeable outcome was that, beams subjected to impact loading experienced a "shear plug" type of failure, with shear cracks around the impact zone, even though the beams were designed as flexure-critical. Beams under static loading showed mostly flexural responses with flexural cracks developing until compression failure for the over-reinforced specimens.

Disciplines

Engineering | Science and Technology Studies

Publication Details

Goldston, M., Remennikov, A. M. & Sheikh, M. Neaz. (2015). Energy absorption and impact response of GFRP reinforced concrete beams. 3rd International Conference on Protective Structures (ICPS3) (pp. 168-176). Australia: University of Newcastle.

ENERGY ABSORPTION AND IMPACT RESPONSE OF GFRP-REINFORCED CONCRETE BEAMS

M.W. Goldston
School of Civil, Mining and Environmental Engineering, University of Wollongong, NSW 2522, Australia.
Email: mwg278@uowmail.edu.au

A.M. Remennikov*
School of Civil, Mining and Environmental Engineering, University of Wollongong, NSW 2522, Australia.
Email: alexrem@uow.edu.au

M.N. Sheikh
School of Civil, Mining and Environmental Engineering, University of Wollongong, NSW 2522, Australia.
Email: msheikh@uow.edu.au

ABSTRACT

It has been demonstrated that glass fibre-reinforced polymer (GFRP) bars is a suitable alternative to traditional steel reinforcement in concrete structures. GFRP bars are a competitive reinforcing option in reinforced concrete members subjected to flexure and shear. GFRP has compelling physical and mechanical properties, corrosion resistance and electromagnetic transparency. The use of GFRP reinforcement is particularly attractive for structures that operate in aggressive environments, such as in coastal regions, or for buildings that host magnetic resonance imaging (MRT) units or other equipment sensitive to electromagnetic fields. However its behaviour under impact loading is not adequately known. This study involved testing a total of twelve GFRP Reinforced Concrete (RC) beams under static and impact loadings and analysing the effect of certain variables including longitudinal reinforcement ratio and concrete strength (normal and high strength). Experimental results confirm that beams with GFRP as internal reinforcement have extremely low post cracking bending stiffness. One noticeable outcome was that, beams subjected to impact loading experienced a “shear plug” type of failure, with shear cracks around the impact zone, even though the beams were designed as flexure-critical. Beams under static loading showed mostly flexural responses with flexural cracks developing until compression failure for the over-reinforced specimens.

KEYWORDS

FRP, RC Beams, Internal Reinforcement, Energy Absorption, Dynamic Equilibrium, Shear

INTRODUCTION

In today’s society, the engineering industry focuses on conventional materials to construct and build resilient structures, including concrete, masonry and steel due to their engineering qualities, such as high tensile strength of steel, compatibility of steel with concrete and overall ductile behaviour. An alternative material that has revolutionised the structural engineering industry is FRP (Fibre Reinforced Polymer). The composite material (FRP) is an attractive substitute for steel due to its superior properties including its non-corrosive behaviour (corrosion is a significant problem for steel when exposed to marine environments), increased durability and low thermal and electric conductivity (ACI-440 2006). Its major attraction is its weight to strength ratio, about 1/5 to 1/4 the density of steel.

Carbon fibre has modernised the engineering world through its ability and properties compared to conventional steel reinforcement. Experimental programs conducted by Rafi et al. (2007), Islam (2009) and Kobraei et al. (2011) used carbon fibre as their main reinforcement material in concrete beams. Their main objective was to understand how influential the CFRP is under monotonic increasing loads. All articles noted the positives associated with the FRP bars compared to steel for the different parameters investigated including cracking load, moment capacity, load-deflection relationship and tensile strain in the reinforcement.

Overall conclusions associated with the research were that the beams with FRP bars as internal reinforcement were capable of sustaining larger load, but deflections were significantly increased due to the low elastic modulus (stiffness) of the material. The significant advantage of using this material is its ability to be applied in structures in aggressive environment which may lead to corrosion of steel reinforcement.

Research of the impact response of structures including steel tubes and concrete columns has been thoroughly investigated by Remennikov et al. (2011) and Remennikov and Kaewunruen (2006). But research of GFRP RC beams under impact loading hasn't currently been studied. From previous research with steel RC beams under dynamic loads, Saatci and Vecchio (2009) designed an experimental program to understand the behaviour of dynmaic equilibrum, by analysing the resistant forces (support reactions and ineritial resistance) against the impact force. This was achieved by applying accelerometers to measure the inertial resistance and applying load cells at the supports to meaure the resistance. The main obervations associated with this research was that, regardless of the shear capcity of the beams, the specimens displayed severe diagonal shear cracking, even if the beams were designed to be flexure – critical. Also, at the first point of contact, the beam was resisted by ineritial reistance before the supports came into play. This was the foundation and basis of the research in this study, but using internal GFRP reinforcement in the beams.

EXPERIMENTAL PROGRAM

Design of Test Specimens

A total of twelve beams, split into two categories depending on the compressive strength of the concrete were casted and tested. Six beams were cast with normal strength concrete (NSC), 40 MPa with the other six were cast with high strength concrete (HSC), 80 MPa. All beams had identical geometrical properties, with a rectangular cross section of 150 x 100 mm and an overall length of 2400 mm. The variables that were experimentally investigated included the longitudinal reinforcement ratio, concrete strength and failure mode. The longitudinal reinforcement ratios used in this study were calculated as approximately 0.5%, 1.0% and 2.0%. The longitudinal reinforcement ratios together, with the area of reinforcement (A_f) are shown in Table 1. Shear reinforcement was provided @ 100 mm centre to centre for all beams. The specimen names are in the form of A-B-C-D, where A is the specified concrete strength ($f'_c = 40$ or 80 MPa), B is the reinforcement bar type (#2S, #3HM or #4HM), C is the reinforcement ratio (0.5%, 1.0% or 2.0%) and D is for the type of loading, static and impact loading (S& I). Six beams were tested under four point bending, whist the remaining six were tested under the drop hammer. Table 1 shows a summary of the test specimen details.

The proposed GFRP reinforced concrete specimens were designed in accordance with ACI-440 (2006). The reinforcement ratio (ρ_f) and the balanced reinforcement ratio (ρ_{fb}) were calculated and shown in Table 1. These comparison of these ratios, allowed the expected failure mode to be determined. From the results obtained, the beams were designed to be under and over reinforced to demonstrate the three different types of failure mode including balanced failure $\left(\rho_f/\rho_{fb} \approx 1\right)$, concrete crushing $\left(\rho_f/\rho_{fb} > 1\right)$ and GFRP rupture $\left(\rho_f/\rho_{fb} < 1\right)$.

Table 1. Test Specimen Details

Specimen Name	$\boldsymbol{A_f}$ (mm^2)	$\boldsymbol{\rho_f}$ (%)	$\boldsymbol{\rho_{fb}}$ (%)	$\boldsymbol{\frac{\rho_f}{\rho_{fb}}}$	$\boldsymbol{f'_c}$ (MPa)	**Predicted Mode of Failure**
40-#2S-0.5-S&I	63.4	0.5	0.36	1.39	40	Balanced
40-#3HM-1.0-S&I	142.6	1.13	0.23	4.9	40	Concrete Crushing
40-#4HM-2.0-S&I	253.4	2.03	0.26	7.8	40	Concrete Crushing
80-#2S-0.5-S&I	63.4	0.5	0.61	0.82	80	GFRP Rupture
80-#3HM-1.0-S&I	142.6	1.13	0.40	2.83	80	Concrete Crushing
80-#4HM-2.0-S&I	253.4	2.03	0.44	4.61	80	Concrete Crushing

Static Testing Procedure

The static beams were placed under a four point bending configuration, in order to allow for a constant moment region between the two loading points (Figure 1). The clear span length was 2 m, with 200 mm over hand per side. Testing was performed using a 900 kN load cell at a loading rate of 1 mm/min. Once loading initiated, cracks were marked at their corresponding load to understand the behaviour of the beam at different load intervals and to obtain a sequence and pattern of the cracks up until ultimate condition. Each specimen had four strain gauges, two attached to the centre of the tensile reinforcement and two located on the top surface of the beam at the midspan. A linear potentiometer was attached to the underside of the specimen at the centre to allow for the vertical displacement of the beam to be measured during loading, with the load cell used to measure the force the beams could sustain under loading.

Figure 1. Experimental Four Point Bending Apparatus

Impact Testing Procedure

The drop hammer (110 kg mass) was attached to a low friction linear bearing, and not completely free falling, thus there was minimal losses due to friction (Figure 2). The drop hammer was lifted up using a motor and cable which included a clutch to allow the mass to brake or stop whenever power was not supplied. The mass was connected to a rope which when pulled in tension, released the hammer from the cable, allowing it to fall onto the impact specimens. A high speed camera was used to capture the point of impact between the drop hammer and beams. The recording rate of the camera was 500 frames per second. A leveller was placed vertically, close to the specimens to allow for the deflection to be approximated using the high speed camera at the midspan. Load cells were placed at the supports to measure the resistance at these points, with a load cell attached to the main drop hammer. Two accelerometers were attached on the right side of the specimen to measure the inertial resistance. The drop hammer was dropped at a height of 1200 mm for all impact test specimens, to allow for other variables including concrete strength and reinforcement ratio to be analysed more thoroughly. The over – reinforced impact specimens were subjected to two strikes of the drop hammer, since after the first drop, the beams still had the structural integrity to sustain another hit.

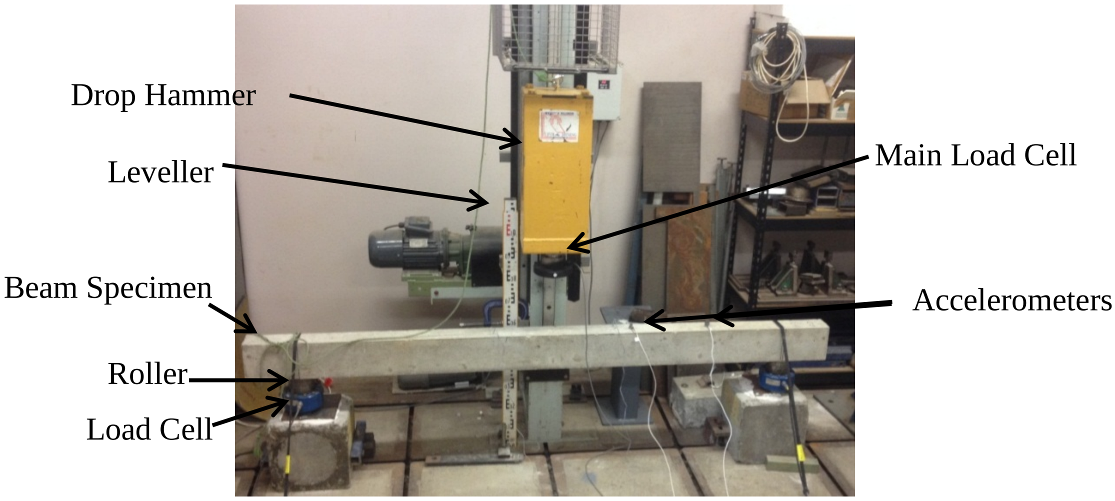

Figure 2. Experimental Impact Test Setup

EXPERIMENTAL RESULTS

Static Tests

The load – deflection behaviour of the six static beams is displayed below in Figure 3. Table 2 displays the experimental static results of all the GFRP RC beams including the initial loading stage at when cracks began to form, that is the cracking load (P_{cr}), the failure load (P_u), which was assumed as the first drop in load carrying capacity for the over reinforced specimens, that is when $\varepsilon_{cu} = 0.003$, experimental moment capacity (M_{exp}) which was calculated using $M_{exp} = P_u L/6$ and experimental deflection (Δ_{exp}), corresponding to P_u.

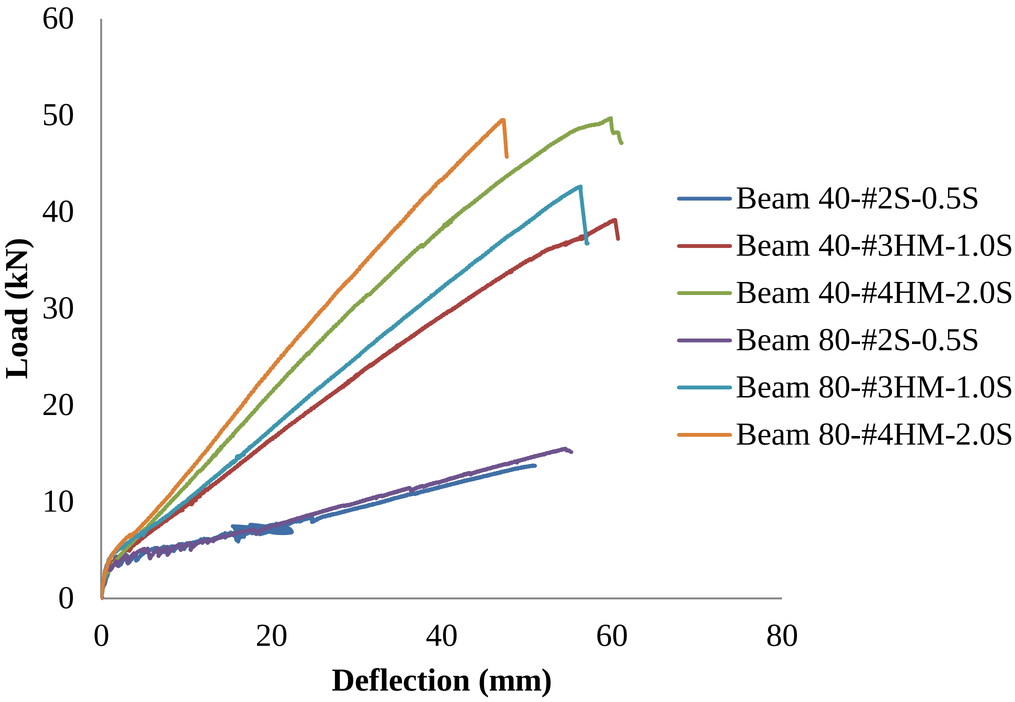

Figure 3. Load – Deflection Behaviour of GFRP RC Beams

Table 2. Experimental Static Test Results

Beam	P_{cr} (kN)	P_u (kN)	M_{exp} (kNm)	Δ_{exp} (mm)	Failure mode
40-#2S-0.5-S	3.0	13.8	4.60	52.2	Balanced
40-#3HM-1.0-S	5.0	39.2	13.1	60.4	Concrete Crushing
40-#4HM-2.0-S	5.8	49.7	16.6	59.9	Concrete Crushing
80-#2S-0.5-S	3.6	15.5	5.17	54.5	GFRP Rupture
80-#3HM-1.0-S	5.9	42.6	14.2	56.3	Concrete Crushing
80-#4HM-2.0-S	5.7	49.5	16.5	47.3	Concrete Crushing

The response of the GFRP RC beams under four point bending displayed pre – and post – cracking behaviour. The load – deflection response was linear up until failure. From Figure 3, the bending stiffness of the beams significantly reduced once cracking initiated. The reason for this is because of the low elastic modulus of the GFRP reinforcement bars. The experimental elastic modulus of the rebars was determined, by carrying out tensile tests on all three different diameter rebars (#2S, #3HM, #4HM), with the average results being 37.5 GPa, 55.6 GPa and 48.6 GPa, respectively. This is significantly lower than for conventional steel, that is 200 GPa. For the test specimens with $\rho_f =$ 0.5%, the beams failed once the ultimate load was reached. There was no prior warning of collapse, with the GFRP reinforcement bars rupturing. Concrete crushing and GFRP tensile ruptured occurred simultaneously at the point of failure for the balanced test specimen as shown in Figure 4. Whereas, for the four over – reinforced specimens, their assumed failure was at $\varepsilon_{cu} = 0.003$ and this occurred in the first drop in load, see Figure 5. The four over – reinforced specimens were able to sustain loading after this, until they collapse due to shear cracking propagating from the supports. The shear capacity was reached, but this occurred after the concrete crushing had occurred. The over – reinforced specimens also displayed higher post – cracking bending stiffness, due to the higher elastic modulus and this is evident from the steeper gradient in the load – deflection relationship.

Crack propagation of all specimens initiated with vertical flexure cracks within the constant moment region before moving towards the supports. These cracks continued to propagate towards the compressive side of the beam. All specimens displayed average crack spacing of approximately 100 mm.

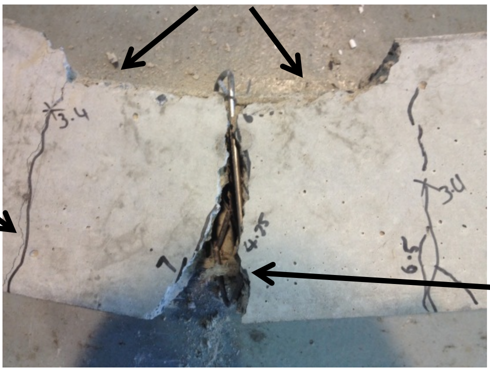

Figure 4. Concrete Crushing and GFRP Tensile Failure (Balanced) of Beam 40-#2S-0.5-S

Concrete crushing in the pure flexure zone at $\varepsilon_{cu} = 0.0029$

Figure 5. Concrete Crushing of Over-Reinforced Beam 40-#3HM-1.0-S

Figure 6 displays a comparison of the energy absorption of the static beams, defined as the area enclosed by the load – deflection curve. The energy absorption before the maximum load is defined as the energy absorption the beam could sustain before displaying a significant drop in load carrying capacity. Whereas, after this point, the beam has essentially failed but it can be seen that all for over – reinforced specimens were capable of handling energy up until total collapse (shear failure). The beams designed to fail by GFRP rupture had no energy after their maximum load was attained. This additional energy absorption after maximum load is attained is a result of concrete confinement phenomena and the ability of the concrete to undergo further strains as the load increased. One observation was that the reinforcement ratio affects the energy absorption more significantly before the maximum load is reached compared to the concrete compressive strength.

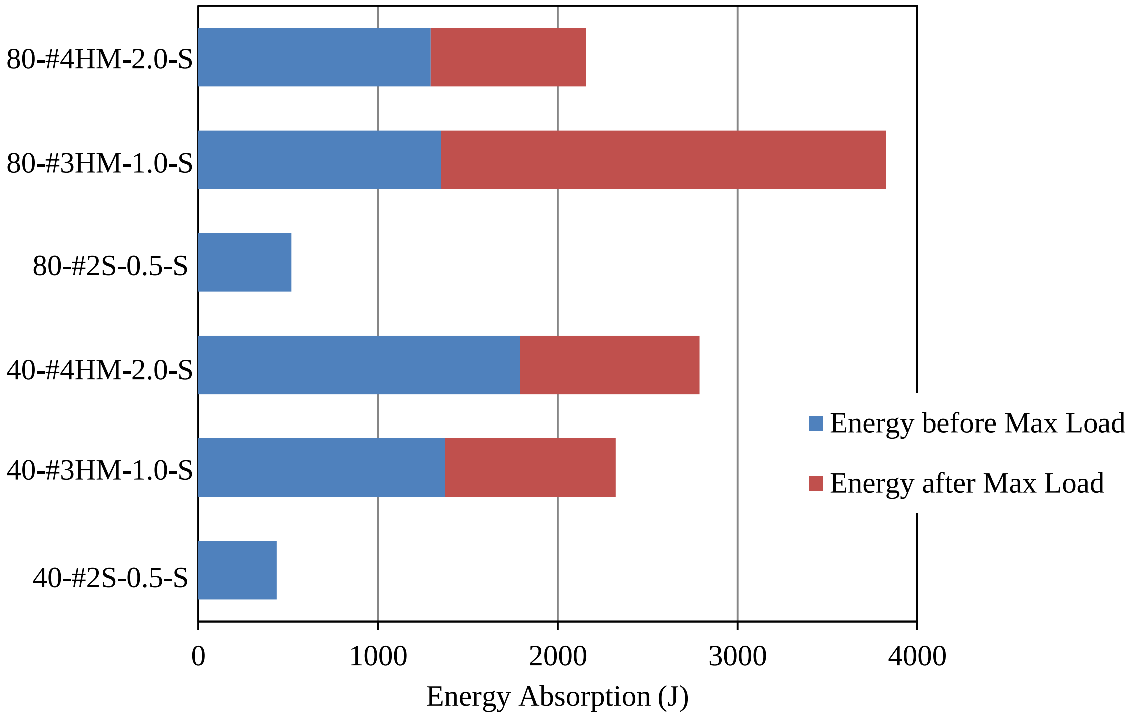

Figure 6. Comparison of Energy Absorption of Static Test Specimens

Impact Tests

Table 3 analyses all forces experienced by the beams to prove and verify dynamic equilibrium. The resistant forces, including the two support reactions as a function of time, $R_1(t)$ and $R_2(t)$ and inertia, $\int_0^L ma(x,t)dx$, which is defined as the inertial resistance, mass of the specimen multiplied by the acceleration as a function of displacement and time along the specimen were determined for a particular point in time, $t = 0.12$ s. The inertial resistance force along the specimen was assumed as the impact force from the drop hammer, $I(t)$ minus the two reaction supports. Midspan deflection (Δ_{exp}) was determined using the high speed camera. Only one strain gauge was used during testing to understand the behaviour of the GFRP tensile reinforcement under impact load (ε_{frp}).

Eq. 1 displays the vertical force equilibrium of a specimen under dynamic forces as a function of time along the beam.

$$\int_0^L ma(x,t)dx + \mathrm{R}_1(t) + \mathrm{R}_2(t) - I(t) = 0 \tag{1}$$

Table 3. Experimental Impact Test Results of GFRP RC Beams

		At $t = 0.12$ s					
Beam	**Drop**	$I(t)$ (kN)	$R_1(t)$ (kN)	$R_2(t)$ (kN)	$\int_0^L ma(x,t)dx$ (kN)	Δ_{exp} (mm)	ε_{frp} (%)
40-#2S-0.5-I	1	18.6	8.31	6.73	3.58	*	*
40-#3HM-1.0-I	1	33.8	14.8	15.1	3.89	57.5	0.95
40-#4HM-2.0-I	1	*	*	*	*	52.3	*
	2	42.9	18.6	19.8	4.49	*	0.78
80-#2S-0.5-I	1	19.8	8.21	9.82	1.77	*	1.24
80-#3HM-1.0-I	1	34.3	14.2	18.3	1.71	51.6	0.96
80-#4HM-2.0-I	1	34.7	19.6	16.3	−1.12	43.8	0.68

* Data not obtained due to malfunctions with operating equipment or inability to determine certain variables (deflection).

As displayed in Figure 7, the graph represents the impact forces and the resisting forces for a 50 millisecond window (from 90 ms to 140 ms) of testing for beam 40-#3HM-1.0-I. It is clear that the first initial contact occurred at 0.1 seconds, by a large spike in the impact force and inertia. It is evident, that at this point in time, the inertia force was approximately equal to the impact force, with the support reactions not being utilised during the initial contact.

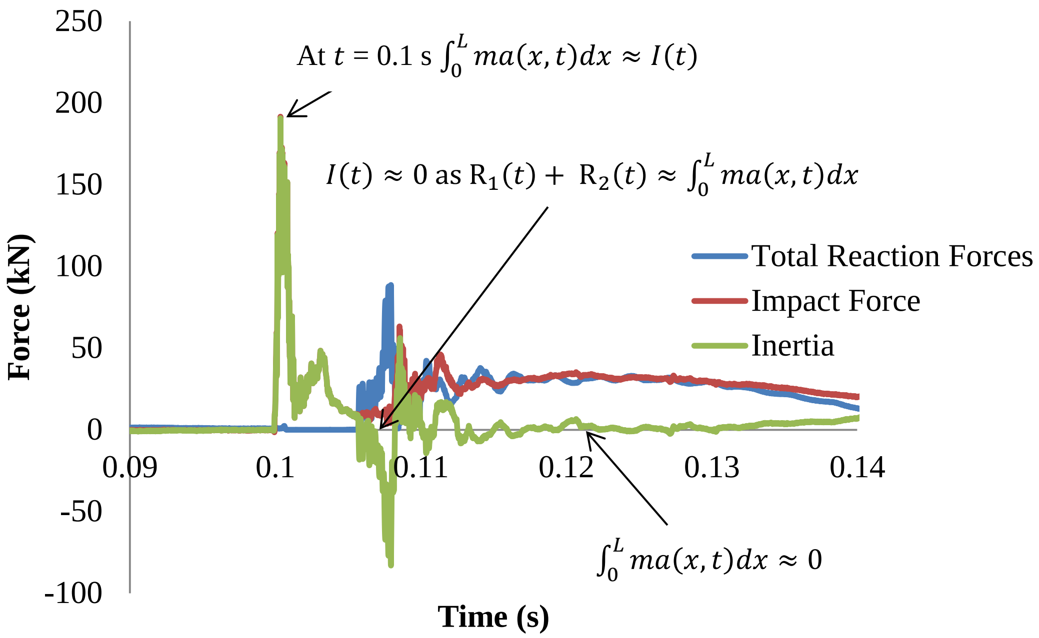

Figure 7. Breakdown of Resisting Forces for Beam 40-#3HM-1.0-I

There is a general pattern from the results, that at the point of contact between the beam and drop hammer; resistance is dependent on the inertia forces. Initially, approximately 100% of the resistance is by the inertia forces. At supports $R_1(t)$ and $R_2(t)$, there is very minimal resistance at $t = 0.1$ s, $R_1(t) + R_2(t) \approx 0$ kN. But at 0.12 seconds, there is a significant change in the resistance and this is also evident in Figure 6 where the inertia graph is roughly travelling along the x – axis, indicating no resistance from the inertia forces at this point in time. After the initial contact, the impact force caused stresses in the beam to run longitudinal to the support regions. Thus after the initial contact, resistance was controlled by the reaction supports, that is and average of 90% resisted by supports and 10% by inertia forces for all impact specimens was determined.

For the GFRP RC static beams, the tests revealed mainly a flexure response, with all beams experiencing vertical flexural cracks before compression failure of the concrete, that is when $\varepsilon_{cu} = 0.003$ was reached for the over – reinforced specimens. Even though the crack patterns for the static test beams displayed shear cracking, this occurred after the assumed concrete strain was reached. The shear capacity of the beams was reached after ε_{cu} was attained.

For the same test specimen, but under impact loading (beam 80-#3HM-1.0-I) as displayed in Figure 8, regardless of their static behaviour, it was evident that being subjected under an impact force caused the beam to behave differently in terms of crack pattern and failure mode. The impact beams designed as over – reinforced displayed a “shear plug” type of failure mode, with diagonal shear cracks being formed around the impact zone at angles of approximately 45 degrees. The shear cracks on either side of the impact point were also observed to be parallel, with some very small and minor flexural cracks observed during the two impact hits. Concrete crushing was displayed within the impact zone caused by the force of the drop hammer.

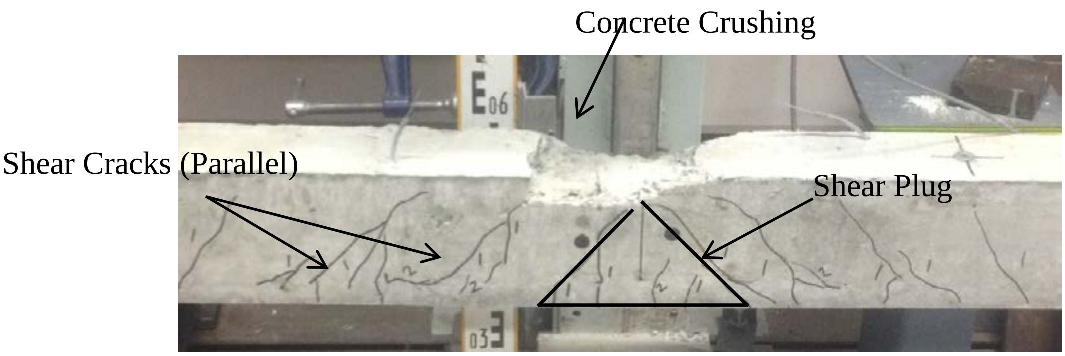

Figure 8. Failure Mode of Beam 80-#3HM-1.0-I under Impact Loading

CONCLUSIONS

A successful experimental program of twelve GFRP RC beams under static and impact loading has been presented and discussed, providing information on the effectiveness of the use of GFRP reinforcement. Observations and experimental data analyses have led to the following conclusions:

1. The failure mode of GFRP RC beams can be accurately predicted by adopting the sectional analysis techniques used for steel reinforcement including the rectangular stress block. The ratio of the reinforcement ratio to the balanced reinforcement ratio (ρ_f/ρ_{fb}) held true for the failure mode of the specimen.
2. Resistant forces were controlled by inertia forces at first contact ($\alpha = 0.99$ at $t = 0.1$ s) before support reactions took the impact load ($\alpha = 0.1$ at $t = 0.12$ s). Thus, the span length of the beam is an important parameter of the structure in resisting the impact forces. The vertical force equilibrium (impact force, inertia resistance, and support reactions) of the specimens at a certain time, $t = 0.12$ s was verified.
3. Regardless of the shear capacity of the impact specimens, the over - reinforced – beams experienced shear cracking under impact loading, around the impact zone. Shear cracks,

formed at approximately 45 degree angles, resulting in a "shear plug" type of failure. This type of failure was different for the static beams, which experienced no shear cracking up until the assumed failure of $\varepsilon_{cu} = 0.003$, but failed in a flexure response with vertical cracks propagating from the tensile region. Thus, the shear behaviour of flexure-critical GFRP RC beams must be considered in dynamic modelling or when designing structures subjected to impact loads. Ignoring the shear mechanisms could results in serious consequences.

ACKNOWLEDGMENTS

The authors would like to acknowledge the technical staff within the High Bay Laboratory including Fernando Escribano, Cameron Neilson and Alan Grant for their contribution and technical support during the project.

REFERENCES

American Concrete Institute (ACI), (2006) "Guide for the design and construction of concrete reinforced with FRP bars", ACI 440.1R-06, Detroit, MI, February 2006.

Islam, A.K.M, A., (2009) "Effective methods of using CFRP bars in shear strengthening of concrete girders", *Engineering Structures*, Vol. 31, No. 3, pp. 709-714.

Kobraei, M., Jumaat, Z.M. and Shafigh, P. (2011) "An experimental study on shear reinforcement in RC beams using CFRP-bars", *Scientific Research and Essays*, Vol. 6, No. 16, pp. 3447-3460.

Rafi, M.M., Nadjai, A. and Ali, F. (2007) "Experimental testing of concrete beams reinforced with carbon FRP bars", *Journal of Composite Materials*, Vol. 41, No. 22, pp. 2657-2673.

Remennikov, A., M., Uy, B. and Kong, S. Ying. (2011) "Response of foam- and concrete-filled square steel tubes under low-velocity impact loading", *ASCE Journal of Performance of Constructed Facilities*, Vol 25, No. 5, pp. 373-381.

Remennikov, A. and Kaewunruen, S. (2006) "Impact resistance of reinforced concrete columns: experimental studies and design considerations" *19th Australasian Conference on the Mechanics of Structures and Materials*, Christchurch, New Zealand, Nov 29 - Dec 1, pp. 817-824.

Saatci, S. and Vecchio, F. J. (2009) "Effects of Shear Mechanisms on Impact Behavior of Reinforced Concrete Beams", *ACI Structural Journal*, Vol. 106, No. 1, pp. 78-86.